



# Electrical energy generation from a large number of microbial fuel cells operating at maximum power point electrical load

N. Degrenne<sup>a,\*</sup>, F. Buret<sup>a</sup>, B. Allard<sup>b</sup>, P. Bevilacqua<sup>b</sup>

<sup>a</sup> Université de Lyon, Ecole Centrale de Lyon, Laboratoire Ampère, 36 Avenue Guy de Collongue, Ecully 69134, France

<sup>b</sup> Université de Lyon, INSA de Lyon, Laboratoire Ampère, 20 Avenue Albert Einstein, Villeurbanne 69100, France

## ARTICLE INFO

### Article history:

Received 8 November 2011

Received in revised form 11 January 2012

Accepted 12 January 2012

Available online 20 January 2012

### Keywords:

Microbial fuel cell

Electrical load

Maximum power point tracking

Energy conversion efficiency

Energy harvesting

## ABSTRACT

Microbial fuel cells (MFCs) convert organic matter into electrical power. For most applications, the electrical-load seen from the MFC can advantageously be controlled by a DC/DC inductive converter. Implementation of a so-called maximum power point tracking (MPPT) control permits to set the operating point of the MFC to optimize power harvesting whatever the actual load. This paper studies the electrical performances of MFCs under maximum power point (MPP) load conditions. Ten similar single-chamber 1.3 L MFCs are constructed and simultaneously tested. For an identical amount of injected organic matter (1 g of acetate), the “perturbation and observation” (P&O) algorithm achieves a best electrical energy production of 985 J electrical power, corresponding to 8.6 % global energy conversion efficiency (ECE). A novel algorithm that regulates MFC voltage to one-third its open-circuit voltage is introduced and compared to the state of the art P&O algorithm. It enables a best conversion efficiency of 7.7 % and promises low-cost effective implementation in silicon DC/DC converters.

© 2012 Elsevier B.V. All rights reserved.

## 1. Introduction

Microbial fuel cells (MFCs) convert organic matter into electrical power. Even though the power densities are still limiting [1], recent research works proved the feasibility to supply low-power electronic devices. In [2], a sediment microbial fuel cell is positioned at the bottom of lake Michigan and supplies a wireless temperature sensor. In order to foresee industrial applications, the electrical power densities delivered by MFCs need to be improved. In this objective, research efforts focus on electrodes materials and catalysts, reactor architectures, bacteria populations and growth, substrate and so forth. The output load from electrical viewpoint is another parameter that directly impacts power production and which is often neglected. It sets the operating point, and as such, the output voltage–current pair and the power. Most published works use a fixed resistor value as a load. It has no physical meaning, because in practical applications, the load will most probably not be nor behave like a fixed resistor. It is therefore important to emulate realistic loads to measure effective performances. Further more, it was demonstrated in [3,4] that load impacts the bacterial communities and the electrical performances in the long term, thus emphasizing the role of the output load.

In some applications, MFCs are directly used to charge capacitors. In the EcoBot-III robot [5], twelve modules consisting of four MFCs in parallel are connected in series (i.e. a total of 48 MFCs) to charge a bank of capacitors. A comparator manages the consumption of the stored energy when the voltage reaches 3 V until it decreases to 2 V, at which point the circuit stops and allows the re-charging of the capacitor bank. The energy is therefore dispensed intermittently in a burst of high-power. In this configuration, the load behaves like a switched and variable resistor. The impact of such a load configuration was investigated in [6]. When MFCs are used to charge condensators this way, the apparent load resistance is not always equal to the resistance permitting the maximum power production.

An inductive DC/DC converter permits to interface the MFC to any load. It can be regulated to control the operating point of the MFC and to constantly adapt the apparent resistance to maximize power production as pictured in Fig. 1. In low-power photovoltaic [7] and thermoelectric applications [8], some converters were presented which include a maximum power point tracking (MPPT) regulation. These converters are not suitable for MFCs because they are designed for different power or voltage level and load characteristic. One of our recent work revealed a DC/DC converter specifically designed to harvest maximum energy from MFCs [9].

Few research studies focus MPPT algorithms for MFCs and demonstrate their ability to harvest more electrical energy. In [10], an original multiunit MPPT algorithm is presented in order to fasten the convergence time. The main drawback is that it requires two

\* Corresponding author.

E-mail address: [nicolas.degrenne@ec-lyon.fr](mailto:nicolas.degrenne@ec-lyon.fr) (N. Degrenne).

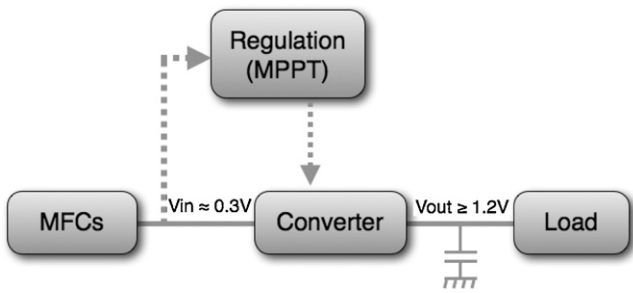


Fig. 1. Harvesting circuit topology including a regulated DC/DC converter.

similar MFCs which is a hard assumptions is such a heterogenous technology. In [11], “perturbation and observation” (P&O), “gradient” and “multiunit” algorithms are compared regarding their robustness to perturbations. The gradient method fails to converge but the P&O proves to be efficient on a variety of MFC applications. Other few research studies investigate the effects of maximum power point (MPP) loading on intrinsic MFCs operation. In [12], acetate-fed MFCs are operated with external resistances, which are above, below, or equal to the internal resistance of a corresponding MFC. Operation with the optimal external resistance (P&O) results in increased power output, improved Coulombic efficiency (CE), and low methane production. In [13], a gradient algorithm improves the electrogenic anodic biofilm selection for power production, indicating that greater power and substrate conversion can be achieved. These results demonstrate the advantage of using MPP loading for energy production and prove that further researches are necessary to evaluate MFCs under these specific load conditions. Additionally, MPP loading eases maximum power real-time monitoring and permits to study MFCs with respect to issues that were never addressed before.

This paper studies electrical power production from acetate for single-chamber MFCs. Different indicators are studied under MPP electrical-load conditions. A first objective is to evaluate the energy conversion from organic matter (acetate in our case) into electricity. In this purpose, Coulombic efficiency (CE) and energy conversion efficiency (ECE) as introduced in [14] are calculated. A second objective is to test a novel so-called MPPT algorithm that regulates the MFC voltage to one-third of the open-circuit value (VREG algorithm). This algorithm is simple, robust and can be effectively implemented in a low-power inductive DC/DC converter as discussed in [9]. Its performances are compared to a state-of-the-art P&O algorithm.

## 2. Materials and methods

### 2.1. Microbial fuel cells

Ten single-chamber batch MFCs were constructed and are referenced in this paper as MFC01 to MFC10. The single-chamber architecture is chosen for the perspectives for higher power density, the decreased risks of clogging and the autonomous aeration of the cathode [15].

MFCs have 1.3 L cylindrical reactors that are built using commercially available low-cost PVC draining tubes. Two air-cathodes are positioned at both edges for an equivalent cathode surface of 186 cm<sup>2</sup>. They are composed of a 30% wet-proofed carbon cloth (Fuel Cell Earth) coated on the external side by 4 layers of PTFE and on the internal side by a catalyst layer with 0.1 mg cm<sup>-2</sup> platinum and nafion as a binder. Layers are coated manually using a paintbrush as described in [16]. Electrical connections are realized by a titanium wire pressed against the cathode internal side. The anode is positioned in the middle. It is composed of two electrically connected graphite fiber brushes (Gordon Brushes).

### 2.2. Load-controlled measurement tool

An original tool was developed to test ten MFCs simultaneously (Fig. 2). It controls the output load (resistances) of each MFCs independently. The resistance range is from 4.7 Ω to 5 kΩ with steps of 4 Ω, plus open-circuit. The voltage is acquired simultaneously.

A functionality permits to automatically sweep the load resistance from high to low value thus realizing automatic acquisition of polarization and power curves. The chosen time step is 5 min in order to permit stabilization of the voltage (low MFC dynamics).

Another functionality permits to control the resistance using a so-called MPPT algorithm and to record the maximum power in real-time. This can be done using a P&O algorithm, or a voltage regulation (VREG) algorithm.

P&O algorithm starts with an arbitrary resistance chosen by the operator (ex. 1 kΩ). After a defined time step of 5 min, it records power and modifies the resistance with a proportional steps of 20 % (ex. 1.2 kΩ). A variable time step enables increased sensitivity for low resistance values. After 5 min, the new power is recorded. If it increased, the MPP is for higher resistance values and the algorithm next compares powers for higher resistances (ex. 1.2 kΩ and 1.44 kΩ). If it decreased, the MPP is for lower resistance values and the algorithm next compares powers for lower resistances (ex. 0.83 kΩ and 1 kΩ).

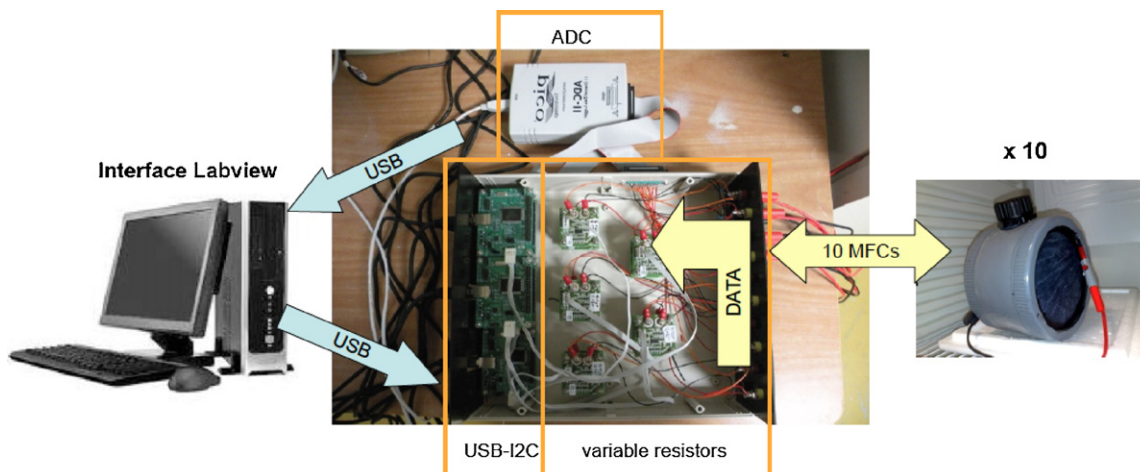


Fig. 2. Measurement tool.

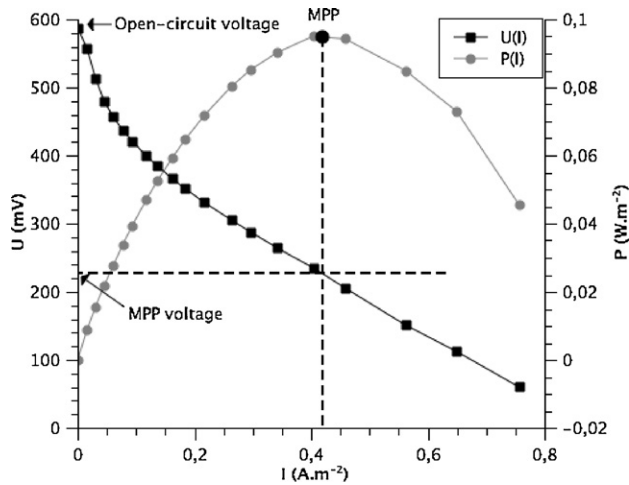


Fig. 3. Polarization and power density curves normalized to the cathode area for MFC04 during EXP3.

VREG algorithm senses the open-circuit voltage every 24 h and controls the load resistance to impose a voltage equal to one-third of the open-circuit voltage (value approximately corresponding to the MPP like presented in Fig. 3). If the voltage is higher, it reduces the resistance by 20%, and if the voltage is lower, it increases the resistance by 20%.

For both algorithms, a limitation is that the optimal output resistance is approached with 20% accuracy what impacts the effectiveness of the electrical production. Decreasing the steps of resistances adversely affects convergence speed.

### 2.3. Protocol

MFCs are simultaneously tested using the load-controlled measurement tool. They are placed in a room where the temperature is regulated at 30°C. Five consecutive experiments are realized.

In EXP1, each MFCs are initially new. They are inoculated with wastewater (Limonest wastewater treatment plant, France) and 1 g of acetate (the initial concentration is therefore 9.4 mMol L<sup>-1</sup>). During inoculation, the load is set to be 1 kΩ for each cell. This experiment lasts 40 days until an electrogenic biofilm develops at the anode and acetate is consumed.

In the two following experiments EXP2 and EXP3, 1 g of acetate is added and the MFCs are tested using the P&O algorithm until acetate is fully consumed.

The objective of the two last experiments EXP4 and EXP5 is to compare VREG to the state-of-the-art P&O algorithm. In EXP4, the five first MFCs (MFC01 to MFC05) constitute the control sample and are tested using P&O algorithm whereas the five last MFCs (MFC06 to MFC10) are tested using VREG algorithm. In EXP5, the five first MFCs (MFC01–MFC05) are tested using VREG algorithm whereas the five last (MFC06–MFC10) are now tested using P&O algorithm.

In between each experiment, water losses are compensated with distilled water. Polarization curves are acquired during experiments.

### 2.4. Calculations

For a given load resistance  $R(\Omega)$  and a measured MFC voltage  $U(V)$  the current  $I(A)$  and power  $P(W)$  are calculated with Eqs. (1) and (2):

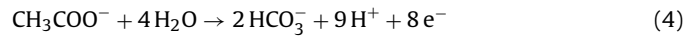
$$I = \frac{U}{R} \quad (1)$$

$$P = \frac{U^2}{R} \quad (2)$$

The Coulombic efficiency (CE) defined in (3) is the fraction of electrons effectively used as current versus the total number of electrons involved in the internal reactions  $n$  (mol).

$$CE = \frac{Q_{\text{effective}}}{Q_{\text{total}}} = \frac{\int I dt}{n \times F} \quad (3)$$

$F$  is the Faraday constant (C mol<sup>-1</sup>). For acetate decomposition in bicarbonate, the theoretical number of electrons involved is 8 as shown in the oxidation and reduction Eqs. (4) and (5), respectively.



1 g of sodium acetate (82.03 g mol<sup>-1</sup>) as used in this experiment theoretically gives  $9.75 \times 10^{-2}$  mol of electrons and therefore a total electric charge  $Q_{\text{total}}$  of 9407.3 C.

The potential efficiency (PE) defined in (6) is the fraction of the potential actually used as output voltage versus the theoretical potential of the involved reaction.

$$PE = \frac{U_{\text{effective}}}{E_{\text{theoretical}}} = \frac{U}{E_{\text{RED}} - E_{\text{OX}}} \quad (6)$$

For the given reaction, the theoretical potential of the reaction is 1.23 V.

PE is a time-dependent value, and we introduce in (7) the equivalent PE ( $PE_{\text{eq}}$ ) which is the average potential of an electron transferred to the anode, and which is expressed as:

$$PE_{\text{eq}} = \frac{\int U \times I \times dt}{\int I \times dt} \times \frac{1}{E_{\text{RED}} - E_{\text{OX}}} \quad (7)$$

The energy-conversion efficiency (ECE) defined in (8) is the fraction of the energy actually harvested from the MFC versus the theoretical energy available through the decomposition of substrate via involved reactions.

$$\begin{aligned} ECE &= \frac{\text{energy output}}{\text{energy theoretically available}} = \frac{\int U \times I \times dt}{n \times F \times (E_{\text{RED}} - E_{\text{OX}})} \\ &= CE \times PE_{\text{eq}} \end{aligned} \quad (8)$$

The energy theoretically available from 1 g of sodium acetate is 11.57 kJ.

## 3. Results

### 3.1. EXP1: biofilm development

During EXP1, the MFCs are inoculated and voltage is recorded during biofilm development. The ten 1.3 L reactors are initially filled with wastewater and 1 g of acetate. The output load is arbitrarily set to 1 kΩ. After 20 days, voltage steps were observed. The amplitude and the length of these steps are very varying from one MFC to another. After 41 days, all ten MFCs consumed the totality of the injected acetate. The voltages drop down to almost 0 V.

### 3.2. EXP2 and EXP3: perturbation and observation algorithm

The objective of EXP2 and EXP3 is to evaluate the performances of the ten MFCs with the state-of-the-art P&O algorithm. Initially starving MFCs are fed with 1 g of acetate. The load resistance of each cell is independently controlled by the P&O algorithm. Electrical characteristics are recorded over time and the experiments are stopped when the total acetate is consumed in all MFCs.

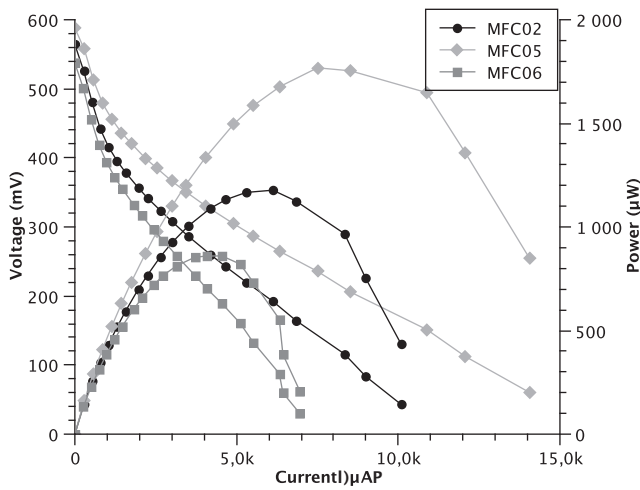


Fig. 4. Typical polarization and power curves of MFCs after 6 days of EXP3.

3.2.1. Experience 2

When acetate is added in the reactors, the power increases sharply (in about 1 day), either straight-after, either with a delay. It corresponds to the activation of the present bacteria with the acetate. Differences are hypothetically due to biofilm maturity. Then, power increases slowly for several days. This phase corresponds to production of electricity by bacteria. Bacteria population are still growing in numbers and therefore enables production of increased power. Finally, power decreases because the substrate concentration in acetate becomes too low.

3.2.2. Experience 3

In EXP3, the registered power curves show that the biofilm is more mature. The power increases sharply straight after acetate addition for all MFCs, and then, the power is more steady than in EXP2. The power levels are higher and the acetate is consumed faster than in EXP2, also meaning that bacteria are more active or in larger number.

Fig. 4 shows typical polarization and power curves that were acquired during EXP3 (only 3 arbitrarily chosen curves are shown in the sake of graph clarity). For each cell, the maximum power measured from the power curves corresponds exactly to the power measured in real-time with the MPPT tool.

The power, voltage and load resistance of an arbitrarily chosen MFC (MFC04) during EXP3 are plotted in Fig. 5. At time  $t_{3A}$ , power increases and load resistance decreases to match the equivalent

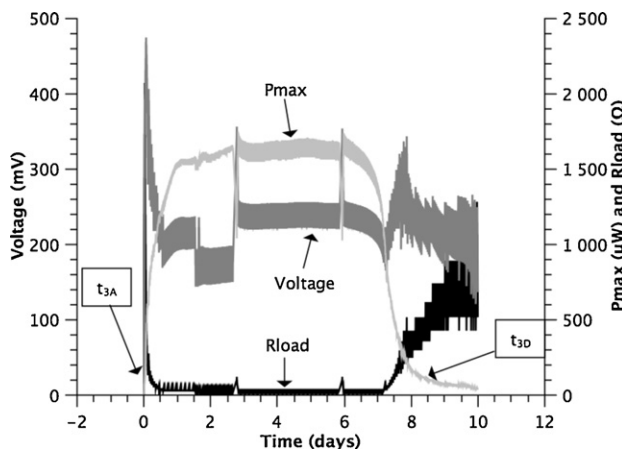


Fig. 5. Load resistance, voltage, and maximum power for MFC04 in EXP3.

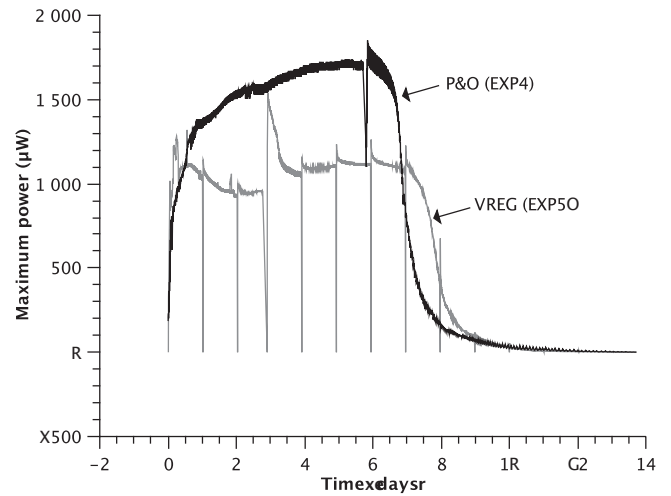


Fig. 6. Maximum power of MFC05 measured using P&O (EXP4) and VREG (EXP5) algorithms.

internal resistance. Voltage is almost constant and equals about 0.2 V. This value corresponds to about one-third of the open-circuit voltage. It comforts the assumption that the maximum power point is achieved through a constant MFC voltage. The apparent dispersion of the voltage curve is caused by voltage variations due to the inherent operation of the P&O algorithm. When acetate is consumed at time  $t_{3D}$ , the power decreases and the load resistance increases. The peak power for MFC04 during EXP3 is defined as the maximum value of the maximum power curve. The produced energy corresponds to the area below the power curve.

3.3. EXP4 and EXP5: comparison of P&O and VREG algorithms

The objective of EXP4 and EXP5 is to compare the ability of P&O and VREG algorithms to harvest electrical energy from the MFCs. In Fig. 6, the power curve of MFC05 is plotted for EXP4 (P&O) and EXP5 (VREG). The curve corresponding to P&O conforms to previous experiments. The curve recorded with VREG algorithm is interrupted every 24 h for 20 min in order to re-set the open-circuit voltage. Power level is significantly lower, indicating either that the biofilm was more performant in EXP4 than in the next experiment, either that the VREG algorithm is less performant.

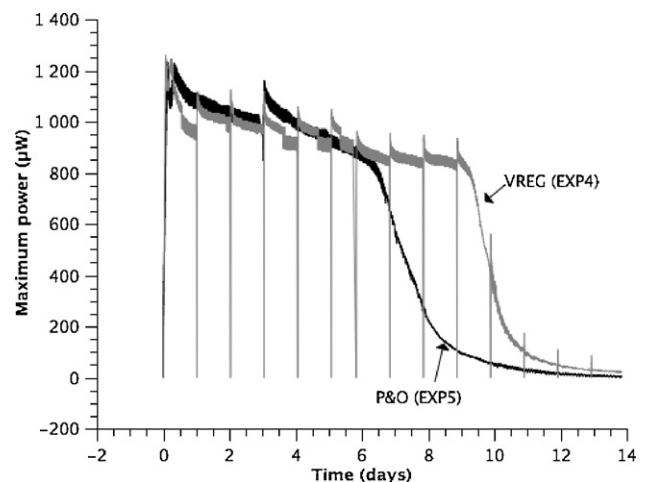


Fig. 7. Maximum power of MFC08 measured using VREG (EXP4) and P&O (EXP5) algorithms.

**Table 1**  
Key values over all the experiments.

	Min energy (J)	Max energy (J)	Average (J)
EXP2	219	633	493
EXP3	510	974	758
EXP4 (P&O)/(VREG)	560/593	985/888	743/712
EXP5 (VREG)/(P&O)	425/411	808/934	588/663
	Min peak power ( $\mu$ W)	Max peak power ( $\mu$ W)	Average ( $\mu$ W)
EXP2	392	1495	888
EXP3	688	1946	1300
EXP4 (P&O)/(VREG)	675/865	1851/1946	1212/1334
EXP5 (VREG)/(P&O)	740/642	2265/2566	1290/1384

In Fig. 7, the power curve of MFC08 is plotted for EXP4 (VREG) and EXP5 (P&O). The curve recorded with VREG algorithm indicates a rather constant power level by over a longer time.

In regards to the differences between the two typical curves under discussion, it is difficult to make serious assumptions on two MFCs only. This is the reason why experiments were largely duplicated. The following discussion considers results of the ten MFCs.

## 4. Discussion

### 4.1. Biofilm development

The resistance value of  $1\text{ k}\Omega$  used during EXP1 is questionable because previous works [12] show that the proliferation of the anodophilic microorganisms was enhanced with low output resistances ( $5\ \Omega$ ).

All MFCs featured a voltage after more than 20 days in presence of bacteria and acetate. This time is long compared to other results cited in the literature [4]. The reason might be found in the materials and glues that were used to fabricate the reactors. They might have inhibited the development of bacteria during the first few days. Another reason can be found in the wastewater that was used for inoculation. Maybe the presence of electrogenic bacteria was limited or parasitic electron acceptors were initially competing with anode. The environment might also have missed minerals or vitamins that are sometimes added during inoculation like in [17].

Table 1 shows that the average energy produced is 494 J in EXP2, to be compared to 758 J in EXP3. The low performances during EXP2 show that the biofilm was not fully developed. A larger part of the organic energy is consumed by bacteria for their own development. Energy conversion rates are better in EXP3 showing that the biofilm is better developed. The conversion rate is overall similar among the five first MFCs in EXP4 compared to EXP3, showing that the biofilm is fully operational after EXP2.

### 4.2. Power and energy production

Average overall peak power is about 1.2 mW. The peak power value is an indicator that must be dealt with carefully. Indeed, peaks of power can happen after a MFC was temporarily stopped for example to draw a polarization curve.

In EXP3, for most cells, the maximum power is stable with time, while substrate concentration decreases. The substrate concentration and power are not linked linearly. It appears that MFCs produce almost identical power for any concentration value above a certain threshold. Power then decreases abruptly when concentration is below the threshold.

Power was constantly acquired through the consumption of acetate. The integration of the maximum power curve versus time was computed to access the electrical energy produced by the MFC.

### 4.3. Energy conversion efficiency

The electrical energy produced can be compared to the theoretical energy available through the full decomposition of acetate like explained in [18,19]. CE and ECE for all MFCs are computed with an uncertainty of 5% corresponding to the precision on the mass of added acetate. CE is 37.4% in average (min 30.1% and max 45.5%). Low values of CE indicate that only a small fraction of the electrons from the reaction are transferred to the anode. ECE is almost proportional to CE and has an average value of 6.2% (min 4.4% and max 8.3%). In EXP3, the best efficiency of 8.3% was achieved for MFC06 for CE = 37.5%. The maximum ECE on all experiment was achieved with MFC04 in EXP4 and is 8.6%.

### 4.4. Dispersions of the performances between cells

All MFCs were built identically in the limit of what is possible to do with the chosen fabrication process. As can be seen in Table 1, the maximum power and energy conversion efficiency are wide spread. For example, in EXP03, the minimum energy is produced by MFC03 (510 J) while the maximum energy is produced by MFC04 (974 J), and the mean value for the ten MFCs is 758 J. All experiment conditions being equal, dispersions between cells result from non-uniform manufacturing processes or microbial heterogeneity during inoculation. Dispersions are the cause of voltage reversal in serial association [20], and are in this regard worth to be evaluated when harvesting energy from a large number of MFCs.

### 4.5. Comparison of the two maximum power point algorithms

With VREG algorithm, MFCs averagely produced 712 J in EXP4 and 588 J in EXP5 whereas with P&O algorithm, MFCs averagely produced respectively 743 J and 663 J. The maximum ECE value with VREG algorithm was achieved with MFC09 in EXP4 and is 7.7%, compared to a maximum ECE of 8.6% with P&O algorithm. Even if P&O algorithm gives overall better experimental results, the differences between the two algorithms does not appear significant with respect of the dispersions between reactors mentioned above.

As a conclusion, the results do not permit to compare both algorithms with precision but permit to evaluate that both algorithms have quite similar efficiencies despite differences in their respective complexity. As a matter of fact, the VREG algorithm, despite its inherent simplicity, can be considered as a good candidate to implement maximum power point tracking on MFCs.

## 5. Conclusions

The use of MPPT algorithm on ten identical single-chamber 1.3 L MFCs permitted to impose a realistic load condition and to constantly measure electrical performances of MFCs. First, the CE and ECE were computed and compared with the intrinsic energy from the injected fuel. A best global substrate conversion efficiency of 8.6% was achieved for the conversion from acetate to electrical energy through microbial fuel cells. Then, a novel MPPT algorithm was introduced and compared to the state-of-the-art P&O method. Best global conversion was 7.7% with this algorithm. A better tuning (time step, resistance step and reference voltage) of VREG algorithm would eventually enable to improve its efficiency while easing the implementation of an output DC/DC converter. The competitiveness of this algorithm being a compromise between the power transfer effectiveness and the implementation efficiency gain compared to its P&O counterpart.

Future works will permit to find the trade-off between maximum power harvesting, and maximum energy conversion efficiency.

## References

- [1] N. Degrenne, F. Buret, B. Allard, J.-M. Monier, *Advanced Materials Research* 324 (2011) 457–460.
- [2] F. Zhang, L. Tian, Z. He, *Journal of Power Sources* 196 (2011) 9568–9573.
- [3] D.Y. Lyon, F. Buret, T.M. Vogel, J.-M. Monier, *Bioelectrochemistry (Amsterdam Netherlands)* 78 (2010) 2–7.
- [4] L. Zhang, X. Zhu, J. Li, Q. Liao, D. Ye, *Journal of Power Sources* 196 (2011) 6029–6035.
- [5] I. Ieropoulos, J. Greenman, C. Melhuish, I. Horsfield, *Artificial Life XII*, MIT Press, 2010, pp. 733–740.
- [6] A. Dewan, C. Donovan, D. Heo, H. Beyenal, *Journal of Power Sources* 195 (2010) 90–96.
- [7] Y. Qiu, C. Van Liempd, B.O. het Veld, P.G. Blanken, C. Van Hoof, *Proceedings of ISSCC, IEEE*, 2011, pp. 118–120.
- [8] K. Win, S. Dasgupta, S. Panda, *Proceedings of ECCE Asia 2011, IEEE*, 2011, pp. 1579–1584.
- [9] N. Degrenne, B. Allard, F. Buret, F. Morel, S.-E. Adami, D. Labrousse, *Proceedings of ECCE, IEEE*, 2011, pp. 889–896.
- [10] L. Woodward, B. Tartakovsky, M. Perrier, B. Srinivasan, *Biotechnology Progress* 25 (2009) 676–682.
- [11] L. Woodward, M. Perrier, B. Srinivasan, P.D. Montre, *AIChE Journal* 56 (2010) 2742–2750.
- [12] R.P. Pinto, B. Srinivasan, S.R. Guiot, B. Tartakovsky, *Water Research* 45 (2011) 1571–1578.
- [13] G.C. Premier, J.R. Kim, I. Michie, R.M. Dinsdale, A.J. Guwy, *Journal of Power Sources* 196 (2011) 2013–2019.
- [14] H.-S. Lee, P. Parameswaran, A. Kato-Marcus, C.I. Torres, B.E. Rittmann, *Water Research* 42 (2008) 1501–1510.
- [15] Z. Du, H. Li, T. Gu, *Biotechnology Advances* 25 (2007) 464–482.
- [16] J. Middaugh, S. Cheng, W. Liu, R. Wagner, *How to Make Cathodes with a Diffusion Layer for Single-Chamber Microbial Fuel Cells*, 2006.
- [17] S. Cheng, B.E. Logan, *Bioresource Technology* 102 (2011) 4468–4473.
- [18] B. Logan, B. Hamelers, R. Rozendal, U. Schrorder, J. Keller, S. Freguia, P. Aelterman, W. Verstraete, K. Rabaey, *Environmental Science and Technology* 40 (2006) 5181–5192.
- [19] J. Larminie, A. Dicks, *Fuel Cell Systems Explained*, 2nd ed., John Wiley & Sons, 2003.
- [20] S. Choi, J. Chae, *Proceedings of MEMS, IEEE*, 2011, pp. 1289–1292.